Results and Discussion

Powder XRD patterns (figure 1) from the preparation of Cu_6Sn_5 indicated the occurrence of Cu_6Sn_5 hexagonal structure (JCPDS card no 02-0713) in all conditions using ethylene glycol (EG) as a solvent but varied in concentration (Table 2) due to the impurity by Sn metal presence. The concentration of Cu_6Sn_5 and Sn phases were calculated as percentage volume fraction by direct comparison method using the integrated intensities of Cu_6Sn_5 (101) and Sn (101) peaks [9]. The calculated volume fractions of Cu_6Sn_5 phase were slightly different in four conditions (EGZn45T0, EGZn10TR, EGZn45T50, and EGZn45TR). However, these small differences may not significantly count as the effect of processing parameters. It is interesting that alloys, such as Cu_6Sn_5 can thermodynamically be produced at this ambient temperature and at this short period of time by this method, which is impossible to occur at this temperature taking into consideration by the phase diagram. However, as the contaminated Sn phase exists, annealing in inert gas atmosphere at about 400°C may be required to improve intermetallic purity. For other observations, only Zn and Cu metals were detected in XRD patterns for the conditions using dimethyl sulfoxide (DMSO) and dimethylformamide (DMF) solvents. The vanished of Cu_6Sn_5 compound in DMSO and DMF conditions can be explained by the possibility of Sn^{2+} ion preferably coordinated with these solvent molecules, which act as ligands, through their oxygen atoms to form stable coordinated ions, $[(CH_3)_4S_2Cl_4O_2Sn]^{4+}$ [10-12]. The formation of these coordinated ions hindered the reduction Sn^{2+} ion to a metal form. Therefore, unreacted Zn powder was remained undoubtedly after the reaction finished.

After XRD data were obtained, the SEM technique for morphological study was employed. SEM micrographs of product powders synthesized from all conditions

for Cu_6Sn_5 are revealed in figure 2. Dendrite particles are found in conditions using EG as a solvent. Plate shape particles were obtained with conditions using DMF and DMSO solvents corresponding to and Cu metal, identified by EDS spectrum. The SEM result, which was in consistency with XRD data, indicated the appearance of the remained Zn metal as equiax white particles located on top of the Cu plates. It should be noted that reaction in DMF and DMSO solvents could not be used to stimulate dendrite intermetallic phase. Due to large distribution of dendrite particle sizes in both conditions (EGZn45TR and EGZn10TR) as illustrated in figure 2, the effect of reducing particle size to dendrite formation is not too diverse to be measured.

The microstructure of the dendrite particles was confirmed by TEM technique. Figure 3 shows the TEM micrographs of dendrite particles synthesized from condition EGZn45TR, EGZn10TR, EGZn45T0, and EGZn45T50. The inserted figures are the consequent selected area diffraction pattern from the dendrite area, which give diffraction spots correspond to the crystallographic planes of Cu_6Sn_5 hexagonal structure. The SAD patterns of both single crystal and polycrystalline suggest crystalline dendritic morphology of Cu_6Sn_5 phase obtained. The previous SEM results illustrate dendrite morphology observed in all conditions using EG as a solvent, which was verified by TEM images associated with SAD patterns as Cu_6Sn_5 compound. Therefore, it can be summarized that intermetallic Cu_6Sn_5 compound prepared by this method is considered to appear as dendritic configuration.

The dendritic growth morphology is of particular importance to the application of the compound materials as a component to the Li ion negative electrode. The high surface area to volume ratio inherent in the dendrite morphology acts to reduce the interface overpotential by reducing the current density. It is not obvious, however, why a dendritic morphology is stabilized in this synthesis method. The 'point effect of

diffusion' is the mechanism that has been considered for stabilizing the dendrite morphology during solidification. However, when electric potentials are involved, there is also a contribution from the point effect of the electric field. The proposal put forth here is that the compound dendrites nucleate on the Zn powder, acting as electrodes for the reduction of the Sn and Cu ions. The proposed mechanism is illustrated in figure 4. The electrochemical overpotential at the solution/precipitate interface will produce an electric field acting to focus the ionic current to the dendrite tip. This idea has been considered previously as a rationalization for dendrite formation during electroplating [13].

Conclusion

The nanometer crystalline dendrite Cu_6Sn_5 powder was successfully synthesized by reacting copper and tin chloride salts with zinc powder in an unreacted polar non-aqueous solvent, such as ethylene glycol. Particle size of zinc powder, a reducing agent, unaffected the size of dendrite particles as well as reaction temperature in the range of 0 to 50°C has unconsiderably effect to the formation of the intermetallic phase. Therefore, the solution route method is the economic, convenience, and powerful technique for making dendritic morphology intermetallic compounds.

Acknowledgement

CMU electron microscopy research and service center is thanked for sample testing. Supported for this work from the Thailand Research Fund (TRF) and The Commission on Higher Education, contract no MRG4680166 is gratefully acknowledged.

References

[1] M. M. Thackeray, J. T. Vaughey, A. J. Kahaian, K. D. Kepler, and R. Benedek, Electrochemistry Communications 1(1999) 111-115.

[2] D. Kepler, J. T. Vaughey, and M. M. Thackeray, Electrochemical and Solid-State Letters, 2(7) (1999) 307-309.

[3] M. M. Thackeray, C. S. Johnson, A. J. Kahaian, K. D. Kepler, J. T. Vaughey, Y. Shao-Horn, S. A. Hackney, ITE Battery Letters Vol. 1, No 1.

[4] J. Yang, M. Winter, and J. O. Besenhard, Solid-State Ioincs, 90 (1996) 281.

[5] J. O. Besenhard, J. Yang, and M. Winter, J. Power Sources, 68 (1997) 87.

[6] D. Kepler, J. T. Vaughey, and M. M. Thackeray, J. Power Sources, 81-82(1999)383-387

[7] R. Janot, D. Guérard, Progress in Materials Science 50(2005) 1-92.

[8] T. Sarakonsri, Ph.D. Thesis, Michigan Technological University, Houghton, (2002).

[9] B. D. Cullity, Elements of X-ray Diffraction, 2nd ed. (Massachusetts, Addison-Wesley, 1977)

[10] C. U. Davanzo, G. Yoshitaka, Journal of the Chemical Society, Dalton Transactions: Inorganic Chemistry 3(1981) 843-6.

[11] C. U. Davanzo, G. Yoshitaka, Inorganica Chimica Acta 60 (1982) 219-22.

[12] L. Coghi, C. Pelizzi and G. Pelizzi, Journal of Organometallic Chemistry, 114(1976) 53-65

[13] Modern Electrochemistry: an introduction to an interdisciplinary area (New York, Plenum Press, 1970).

Figure Captions

Figure 1 Powder XRD patterns from the synthesized of Cu_6Sn_5 with conditions EGZn45TR, EGZn10TR, DMFZn45TR, DMSOZn45TR, EGZn45T50, and EGZn45T50

Figure 2 SEM micrographs from the synthesized of Cu_6Sn_5 with conditions (a) EGZn45TR, (b) EGZn10TR, (c) DMFZn45TR, (d) DMSOZn45TR, (e) EGZn45T50, and (f) EGZn45T0

Figure 3 TEM micrographs from the synthesized of Cu_6Sn_5 with conditions (a) EGZn45TR, (b) EGZn10TR, (c) EGZn45T0, and (d) EGZn45T50

Figure 4 Schematic diagram of the mechanism of the dendrite nucleation

Tables

Table 1 Processing parameters for the synthesis of Cu_6Sn_5 compound

Reaction	Solvent types	Particle size of Zn(μ)	Temp (°C)
EGZn45TR	EG	45	Room
EGZn45T0	EG	45	0
EGZn10TR	EG	10	Room
EGZn45T50	EG	45	50
DMSOZn45TR	DMSO	45	Room
DMFZn45TR	DMF	45	Room

Table 2 Percentage calculated volume fraction of Cu_6Sn_5 and Sn phases from XRD data using integrated intensities of Cu_6Sn_5 (101) and Sn (101) peaks

Reaction	Volume Fraction (%) Cu_6Sn_5: Sn
EGZn45TR	97.48 : 2.52
EGZn10TR	99.66 : 0.34
EGZn45T0	99.73 : 0.27
EGZn45T50	99.50 : 0.50

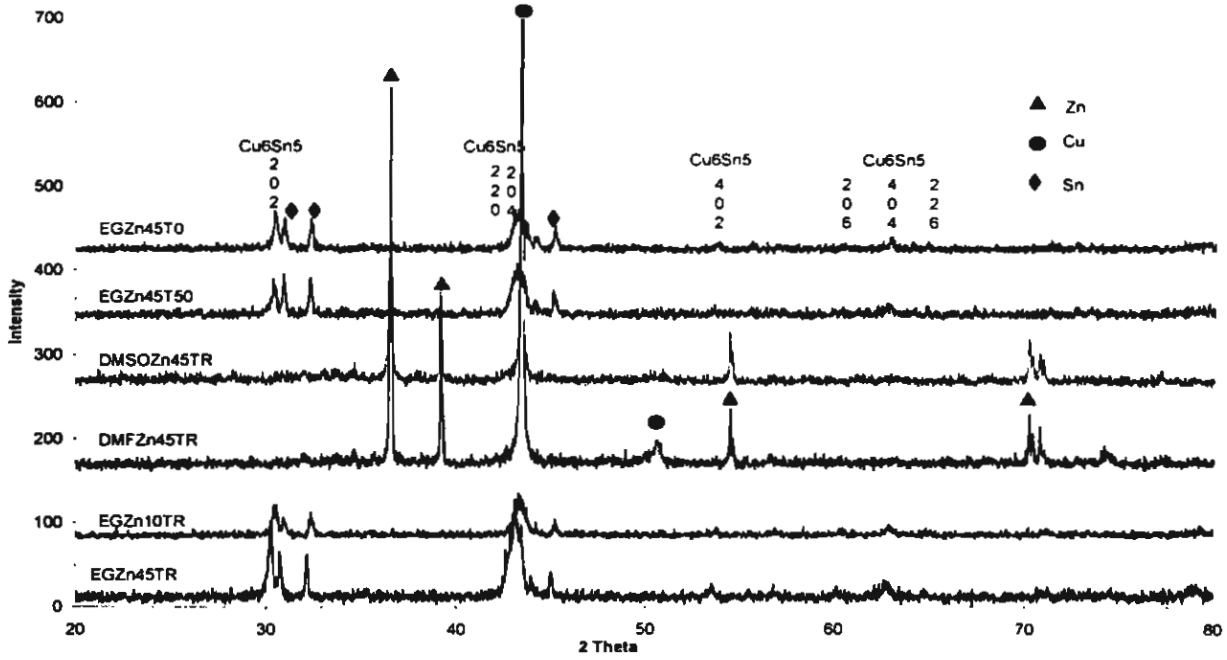
700
600
500
400
300
200
100
0
Intensity
Cu6Sn5
2 0 2
Cu6Sn5
2 2 0
0 4
Cu6Sn5
4 0 2
Cu6Sn5
2 4 2
0 0 2
6 4 6
Zn
Cu
Sn
EGZn45T0
EGZn45T50
DMSOZn45TR
DMFZn45TR
EGZn10TR
EGZn45TR
20
30
40
50
60
70
80
2 Theta

Figure 1

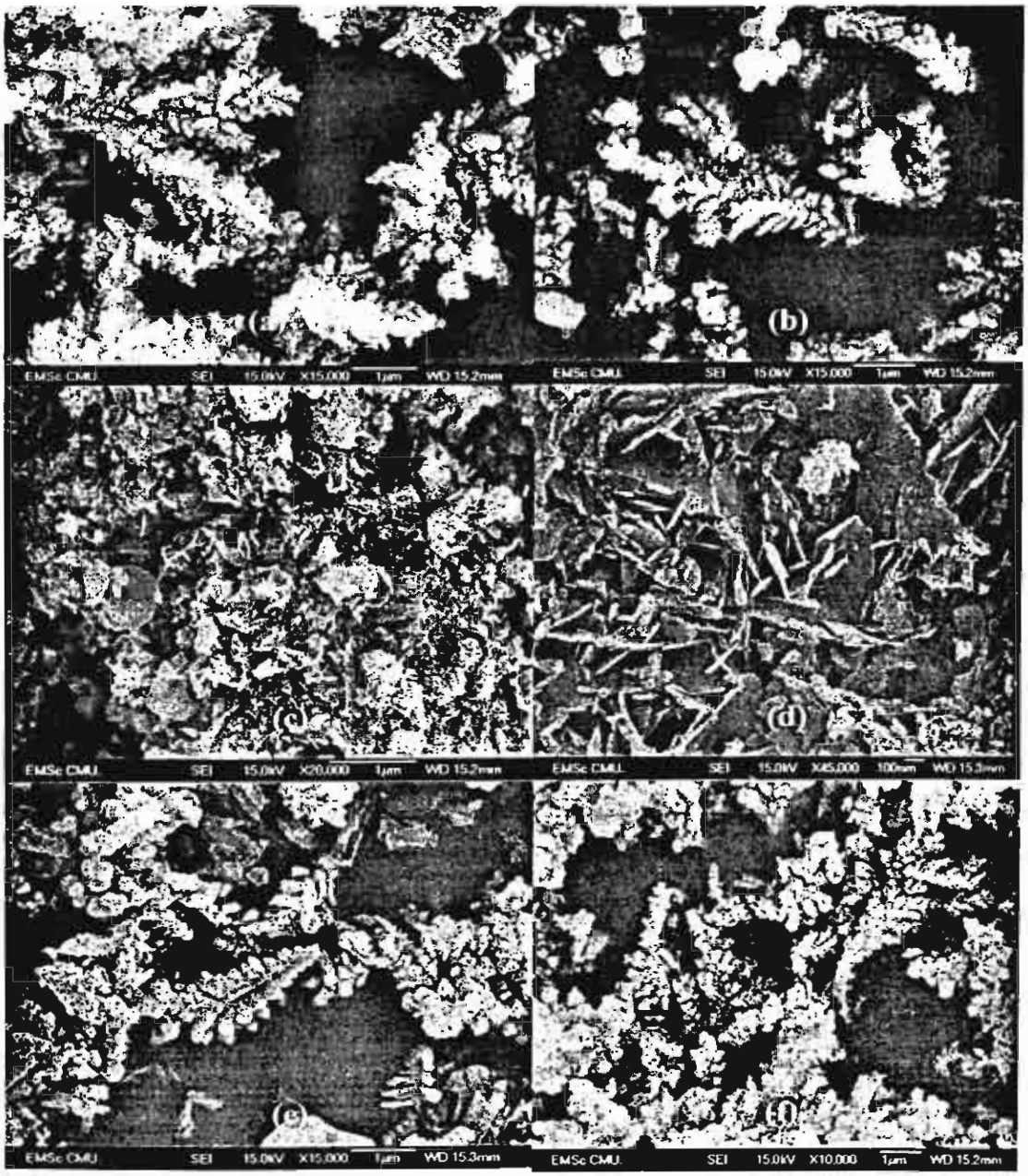

Figure 2

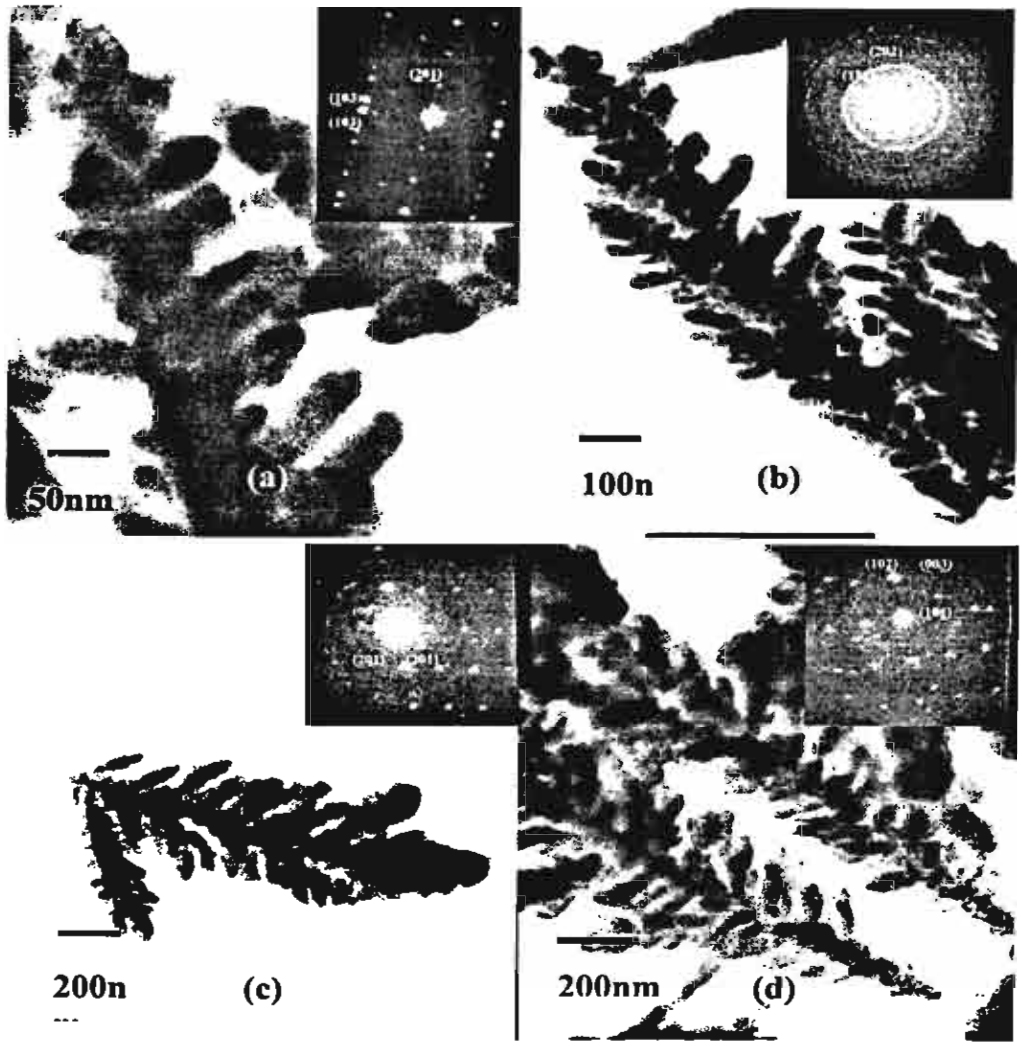

Figure 3

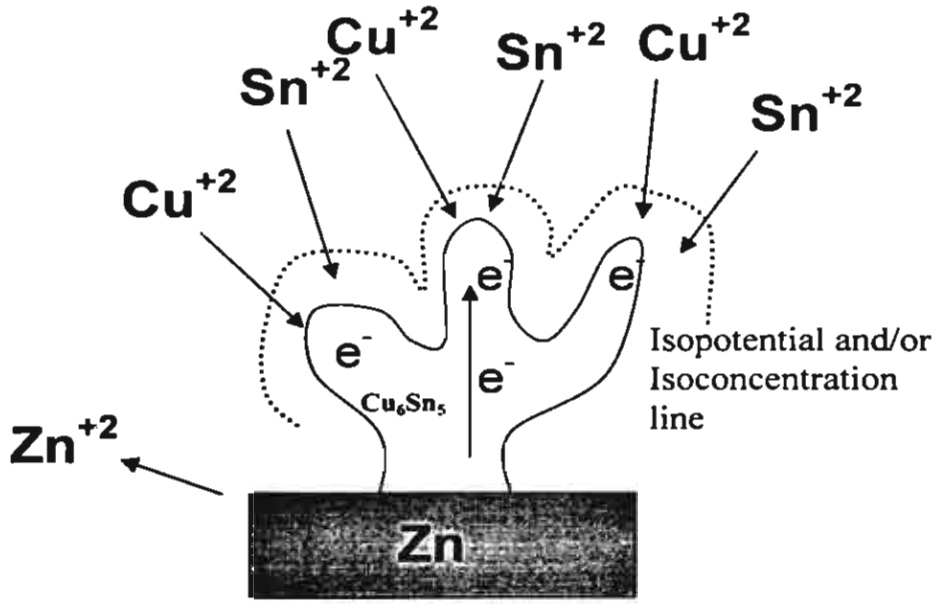
Cu+2
Sn+2
Cu+2
Sn+2
Cu+2
Sn+2
e-
e-
e-
e-
Cu6Sn5
Isopotential and/or
Isoconcentration
line
Zn+2
Zn

Figure 4

Another Investigation: Solution Route Synthesis of Dendrite Cu_2Sb powders, Anode Material for Lithium-ion Batteries

T. Sarakonsri[a*], T. Aamchikad[a], T. Tunkasiri[b]

[a]*Department of Chemistry, Chiang Mai University, Chiang Mai 50200, Thailand*
[b]*Department of Physics, Chiang Mai University, Chiang Mai 50200, Thailand*

Abstract

Dendrite Cu_2Sb powders, anode materials for lithium-ion batteries, was successfully synthesized by redox reaction between metal chloride salts and metallic reducing agent at ambient temperature. This experiment reports on the consequence of processing parameters to the formation of dendrite Cu_2Sb powder. The results from XRD, SEM, and TEM techniques suggest that high purity dendrite Cu_2Sb powder can be synthesized in ethylene glycol by using zinc powder reducing agent at reaction temperature ranging from room to 50°C.

Keywords; Lithium-ion batteries, intercalation compounds, synthesis, electron microscopy, Copper antimonide

* Corresponding author. Tel: +66-53-941907; Fax: +66-53-892277
Email address: scchi017@chiangmai.ac.th;

Introduction

The tetragonal copper antimonide, Cu_2Sb (space group P4/nmm) has been proposed as a potential anode material for lithium-ion batteries with the possibility that lithium can be intercalated in its structure [1]. High gravimetric capacity (about 290 mAh g^{-1} or about 1914 mAh cc^{-1}) and excellent capacity retention were received from this electrode [2]. The preparation of Cu_2Sb compound can be carried out by conventional ball-milling process or by pulse laser deposition method [3-5]. Due to the concerning of particle size and nanotechnology come to play an important role in this part, recently the economical and less time consuming method to prepared nanocrystalline intermetallic Cu_6Sn_5 compound has been introduced [6]. Solution route or oxidation-reduction method was reported for the production of Cu_6Sn_5 with dendritic morphology. The intermetallic compound was received by performing in ethylene glycol, using 10 and 45μm zinc powder, and at reaction temperature up to 50°C. Nanocrystalline intermetallic Cu_2Sb compound additionally has been synthesized in this way and was reported for using as anode material for lithium-ion batteries [7-9]. There were several processing parameters that had to be controlled to acquire the most suitable means to synthesize this material; such as solvent, reducing agent, and temperature. Therefore, this experiment will explore the consequence of those processing parameters to dendrite Cu_2Sb powder formation in order to obtain the most suitable means to produce crystalline dendrite Cu_2Sb powder.

Experimental

The theory concerning solution route synthesis was described in the report on dendrite Cu_6Sn_5 powders [9]. For Cu_2Sb compounds, the processing parameters affecting dendrite formation are solvents, reducing agents, reducing agent particle sizes, and reaction temperatures. Only one type of solvent was examined which is

ethylene glycol (EG, JT. Baker, purity 99.0%) From the previous study, EG solvent initiated more suitable for synthesizing dendrite intermetallic powder over other two solvents (dimethyl sulfoxide, DMSO and dimethyl formamide, DMF) [6]. Zinc (Fluka, 10 and 45μ particle size) was used as reducing agent along with magnesium (Sigma-Aldrich, purity 99.0%), which has more negative value of standard reduction potential than zinc. The reaction temperature at 0°C, room, and 50°C were employed.

The preparation of Cu_2Sb was conducted and coded according to the processing parameters as shown in table 1. The detail of the preparation for the first experimental condition was carried out by dissolving stoichiometric amounts (equation (1)) of $CuCl_2$ (Sigma-Aldrich, purity 99.0%) and $SbCl_3$ (Aldrich Chemical, purity 99.0%) in ethylene glycol at room temperature. Zinc powder was gradually added to the solution. The reaction was continuously stirred for over 1 hour before it was filtered and washed by methanol (Merck, commercial grade). Finally, it was dried in the oven at 65°C for 30 minutes.

$$2CuCl_2 + SbCl_3 + 3.5Zn \rightarrow Cu_2Sb + 3.5ZnCl_2 \qquad (1)$$

As received powders were characterized for the phases presented by powder X-ray diffraction (XRD, siemen D500/D501, Cu Kα (λ1.54) Ni filter, 2θ = 10-80°, step:0.02°, step time: 1s) technique. Scanning Electron Microscopy (SEM) equipped with Energy Dispersive Spectroscopy (EDS) (JEOL JSM-6335F) technique was used to observe morphology of the product powders. Finally, nanometer scale morphology which directly related to the crystallography of the phase presented was determined by Transmission Electron Microscopy (TEM) equipped with Energy Dispersive Spectroscopy (EDS) (JEOL JEM-2010) technique.

Results and Discussion

The X-ray diffraction patterns and SEM images of the as received powders for all synthesis conditions were illustrated in figure 1 and 2, respectively. TEM analyses of selected conditions were demonstrated in figure 3. The major phase presence was identified to be tetragonal Cu_2Sb phase (JCPDS card no 85-492) for all synthesis conditions with some small amount of impurities as indicated in figure 1. It was observed that sharpest XRD peaks were obtained in EGZn45TR condition. Its SEM image (figure 2a) revealed number of relatively small dendrite particles being nucleated out of agglomerated rounded particle (1μm in diameter); assemble the sea anemones in nanometer scale. By EDS study, analogous copper and antimony signals were observed from both areas suggesting the possibility of rounded morphology being transformed into dendrite. Form the TEM analysis (figure 3a), mostly small dendrite particles were observed. These dendrites hence were assumed to be former attached to those large particles observed in SEM image which they were separated out by the TEM sample preparation process. The selected area diffraction (SAD) ring pattern in the inserted figure corresponds to tetragonal Cu_2Sb. However, there was a thin film area which its SAD pattern corresponded to copper was discovered as well as the area of copper plus zinc metals (confirmed by the EDS spectrum) and its corresponding SAD pattern (figure 3a) belongs to ε-$CuZn_3$ phase [10-11] which appeared in XRD pattern at 36.24 and 41.95 degree 2θ. Therefore, some antimony metal remained unreacted and evident in the XRD pattern. It was noted that the volume fraction could not accurately calculated due to peaks overlapping in XRD patterns.

For EGZn10TR, EGZn45T50, and EGZn10T50 conditions, mostly dendrite particles were observed (figure 2b-2d), which is relatively smaller compared to

rounded particles in EGZn45TR. Consequently, broad peaks which appeared in XRD patterns may assumed as because of small particle size effect [12]. The TEM analyses of these conditions were in good agreement with SEM data for relatively larger dendrite particles than observed in EGZn45TR. The (1$\underline{1}$0) zone axis single crystal SAD pattern of EGZn10TR (figure 3b) was shown in the inserted figure representing high crystalline Cu_2Sb dendrite. For condition EGZn10T50, the (10$\underline{1}$) zone axis single crystal SAD pattern (figure 3c) of the Cu_2Sb dendrite particle was observed as well. There were no areas of thin copper and $CuZn_3$ film as observed in EGZn45TR.

The reactions reacted at 0°C (EGZn45T0 and EGZn10T0) reveal very broad XRD peaks suggesting the possibility of amorphous phase presence. The SEM results show the major morphology of large agglomerated particles (figure 2e and 2f) suggesting amorphous phase which is in accordance with the very broad peaks observed in XRD pattern. From these results, it can be concluded that product crystallinity and purity perhaps depend on reaction temperature. Because of an exothermic process, it was observed that using 10μ reducing agent at room temperature generate more heat than using 45μ. Consequently, equilibrium electrons diffusion process occurred, which was resulted in complete growth of dendrite structures. This explanation was applied for the reaction at 50°C additionally. The 0°C reaction produced mostly Cu_2Sb amorphous phase, which was understood to be insufficient energy for diffusion process. However, anealing the product powders under argon atmosphere may improve the crystallinity [8].

The reaction using magnesium reducing agent powder produced mostly agglomerated unwell defined particles (figure 2g) with some dendrite morphology (figure 2h). Furthermore, broad XRD peaks appeared in this reaction, which was assumed to be small particle size effect and more importantly the feasibility that the

magnesium prefer to tetrahedral coordinated by organic group [13] to form organometallic compound through oxygen atoms of ethylene glycol molecules. Although it has more negative standard reduction potential value, reaction in organic solvent might not applicable.

Conclusion

The tetragonal Cu_2Sb was successfully synthesized by solution route method. Reaction temperature and reducing agent particle size has an effect on dendrite particle formation and crystal characteristic. The reaction using zinc 10μm powder at room temperature and the reactions at 50°C produced the most purified crystal Cu_2Sb dendrite powders.

Acknowledgement

The Chiang Mai University electron microscopy research and service center is thanked for sample testing. Support for this work from the Thailand Research Fund (TRF) and The Commission on Higher Education, contract no MRG4680166 are gratefully acknowledged.

References

[1] R. Benedek and M. M. Thackeray, Journal of Power Sources, 110(2002) 406-411

[2] M. M. Thackeray, J. T. Vaughey, C. S. Johnson, A. J. Kropf, R. Benedek, L. M. L. Fransson, and K. Edstrom, Journal of Power Sources, 113(2003) 124-130

[3] M. Kis-Varga and, D. L. Beke, Materials Science Forum (1996), 225-227(Pt.1), 465-470

[4] L. M. L. Fransson, J. T. Vaughey, R. Benedek, K. Edstrom, J. O. Thomas, and M. M. Thackeray, Electrochemistry Communications, 3(2001) 317-323

[5] Seung-Wan Song, R. P. Reade, E. J. Cairns, J. T. Vaughey, M. M Thackeray, and K. A. Striebel, Journal of the Electrochemical Society (2004), 151(7)

[6] T. Sarakonsri, T. Apirattanawan, S. Tungprasurt and T. Tunkasiri, Submitted to Journal of Materials Science

[7] C. S. Johnson, T. Sarakonsri, S. A. Hackney, J. T. Vaughey, N. Li, and M. M Thackeray, presented at 2004 IBA Battery and Fuel Cell materials Symposium, Graz, Australia, April 18-22, 2004

[8] T. Sarakonsri, C. S. Johnson, J. T. Vaughey, N. Li, S. A. Hackney, and M. M Thackeray, presented at 12th International Meeting on Lithium Batteries (IMLB-12), Nara, Japan, June 27-July 2, 2004

[9] T. Sarakonsri, Ph.D. Thesis, Michigan Technological University, Houghton, (2002)

[10] R. Juskenas, V. Pakstas, A. Sudavicius, V. Kapocius, and V. Karpaviciene, Applied Surface Science 229(2004) 402-408

[11] R. Juskenas, V. Latvys, Chemija, 1(1992)54-66

[12] B. D. Cullity, Elements of X-ray Diffraction, 2nd ed. Massachusetts, Addison-Wesley, 1977

[13] A. G. Sharpe, Inorganic Chemistry, 2nd ed. Singapore, Longman, 1986

Figure Captions

Figure 1 Powder XRD patterns from the synthesized of Cu_2Sb with conditions EGZn45TR, EGZn10TR, EGZn45T50, EGZn10T50, EGZn45T0, EGZn10T0, and EGMgTR

Figure 2 SEM micrographs from the synthesized of Cu_2Sb with conditions (a) EGZn45TR, (b) EGZn10TR, (c) EGZn45T50, (d) EGZn10T50, (e) EGZn45T0, (f) EGZn10T0, (g) EGMgTR for low magnification, and (h) EGMgTR for high magnification

Figure 3 TEM micrographs from the synthesized of Cu_2Sb with conditions (a) EGZn45TR showing dendrite particles and its corresponding SAD pattern which corresponds to Cu_2Sb compound, thin film area which its SAD ring pattern belongs to copper metal and copper plus zinc area which its SAD pattern corresponds to ε-$CuZn_3$ phase, (b) EGZn10TR, and (c) EGZn10T50

Tables

Table 1 Processing parameters for the synthesis of Cu_2Sb compound

Reaction	Solvent types	Particle size of Zn(μ)	Temp (°C)
EGZn45TR	EG	45	Room
EGZn10TR	EG	10	Room
EGZn45T50	EG	45	50
EGZn10T50	EG	10	50
EGZn45T0	EG	45	0
EGZn10T0	EG	10	0
EGMg45TR	EG	Mg	Room

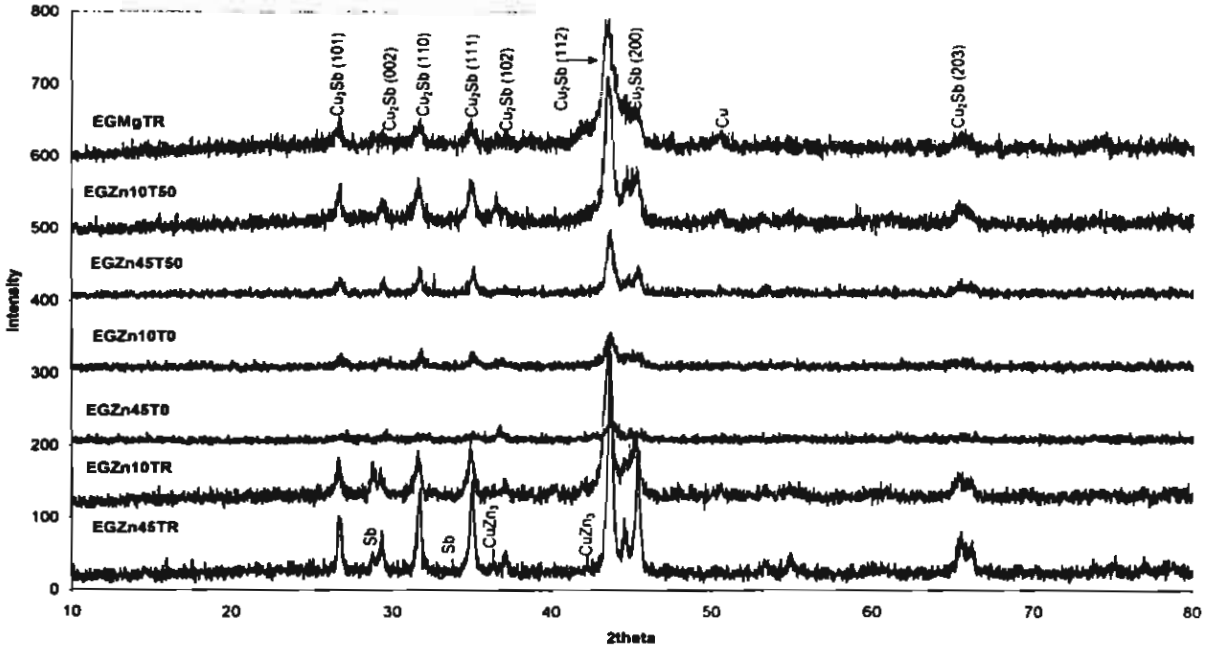
Intensity
2theta
EGMgTR
EGZn10T50
EGZn45T50
EGZn10T0
EGZn45T0
EGZn10TR
EGZn45TR
Cu3Sb (101)
Cu3Sb (002)
Cu3Sb (110)
Cu3Sb (111)
Cu3Sb (102)
Cu3Sb (112)
Cu3Sb (200)
Cu
Cu3Sb (203)
Sb
Sb
CuZn3
CuZn3

Figure 1

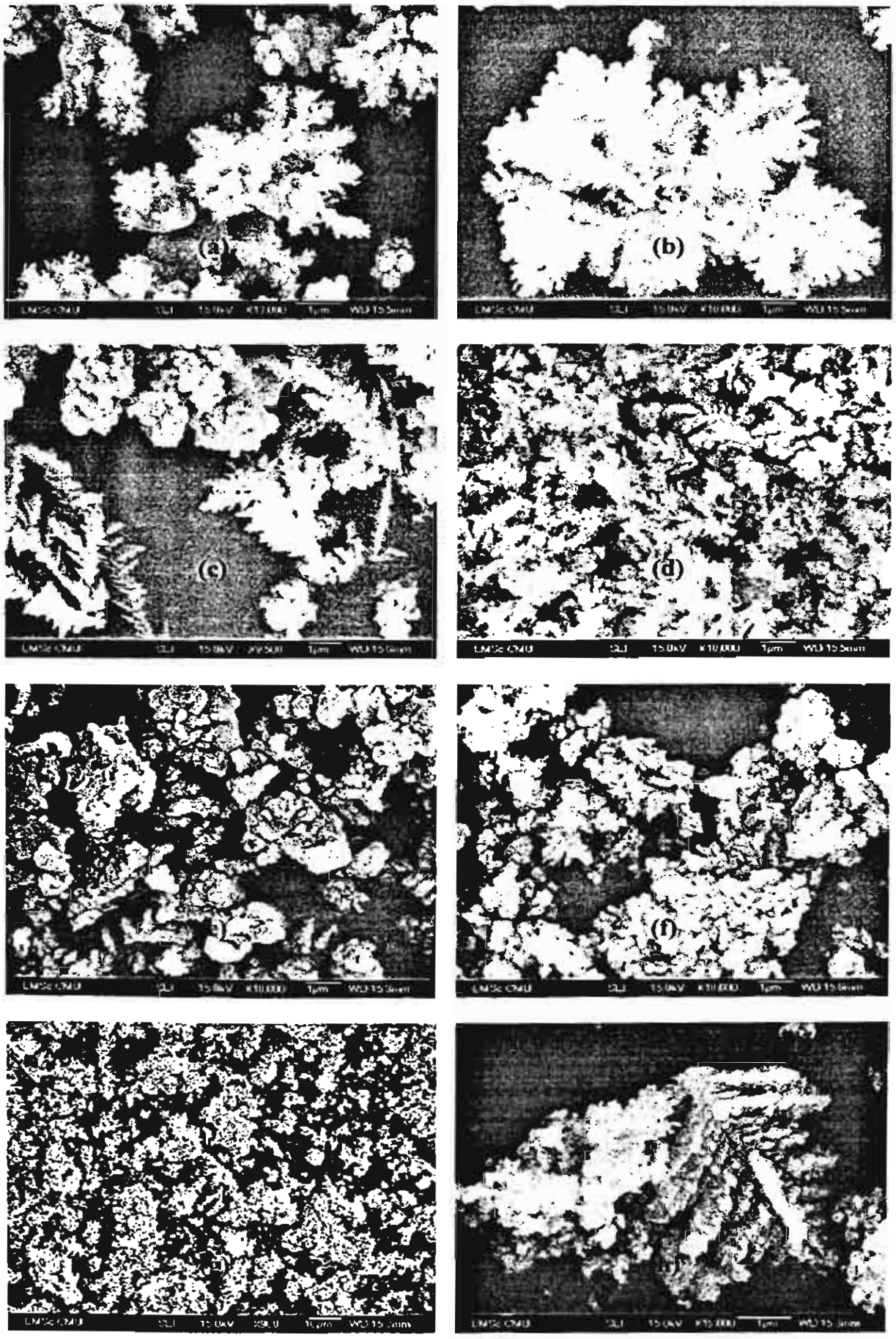

Figure 2

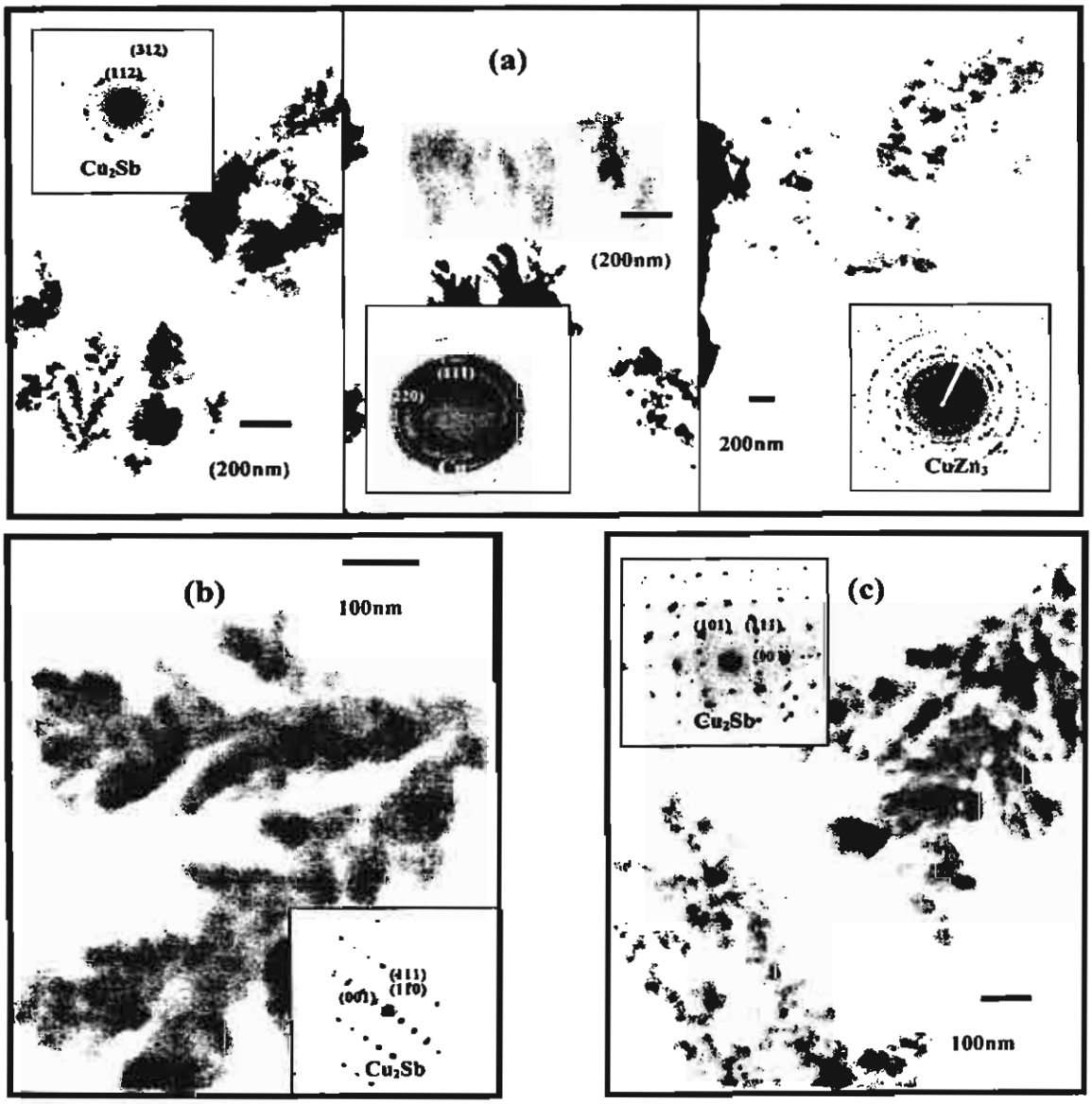
(312)
(112)
Cu2Sb
(200nm)
(a)
(200nm)
(111)
(220)
200nm
CuZn3
(b)
100nm
(411)
(110)
(001)
Cu2Sb
(c)
Cu2Sb
100nm

Figure 3

Solution Route Preparation and Characterization of Dendrite InSb powders, Anode Material for Lithium-ion Batteries

T. Sarakonsri[a*], K. Choksawatpinyo[a], S. Seraphin[b], T. Tunkasiri[c]

[a]*Department of Chemistry, Chiang Mai University, Chiang Mai 50200, Thailand*
[b]*Department of Materials Science and Engineering, University of Arizona, Tucson, Arizona, 85721, USA*
[c]*Department of Physics, Chiang Mai University, Chiang Mai 50200, Thailand*

Abstract

Solution route method can be used to synthesize InSb compound, potential anode material for lithium-ion batteries. Stoichiometric amount of $InCl_3$, $SbCl_3$, and Zn powders were reacted in ethylene glycol to receive intermetallic InSb powders. The characterization of the as received product by XRD technique indicated 48% InSb volume fraction and some other impurities. From SEM results, the morphology of the product was observed to have dendritic structure. The selected area diffraction (SAD) pattern obtained from TEM technique verified the dendrite particles as InSb phase. High crystallinity InSb dendrite was also confirmed by TEM micrograph and its single crystal SAD pattern.

Keywords; Lithium-ion battery, intercalation compound, synthesis, electron microscopy, indium antimonide

* Corresponding author. Tel: +66-53-941907; Fax: +66-53-892277
Email address: scchi017@chiangmai.ac.th;

Introduction

The binary semiconducting compound InSb, with zinc-blende type structure (space group F$\bar{4}$3m (216)) has exhibited interesting properties a negative insertion material for lithium-ion batteries replacing graphite electrode for the safety reason [1-3]. Crystallographically, the zinc-blende framework also contains three dimensional interstitial sites suitable for lithium ions intercalation [3]. It was reported that InSb electrode prepared by ball-milling method provides approximately 340 mAh g^{-1}, which was relatively high compared to carbon base electrode [2]. However, the material producing by ball-milling process may introduce some residual stresses as well as particles agglomeration, which potentially reduce the cell performance [4]. Chemical route approach was then came into attention and was proposed [5] with the objective to minimize those problems and more importantly the production cost. The theory concerning this method was reported else where, which analogous to the synthesis of Cu_6Sn_5 and Cu_2Sb compounds [5-7]. From those preliminary results, the intermetallic compounds were observed to precipitate out as dendritic morphology. This morphology appeared to compose of nanometer particles, which associated with high surface area. Consequently, this experiment explored the synthesis of InSb compound by carried the reaction out using only one condition as for the synthesis of Cu_6Sn_5 and Cu_2Sb compounds, which were ethylene glycol solvent, zinc power (45μm particle size) reducing agent, and reacted at room temperature. X-ray diffraction (XRD), scanning electron microscopy (SEM), and transmission electron microscopy (TEM) techniques were employed for phase identification and morphological studied.

Experimental

The preparation of InSb was conducted by dissolving stoichiometric amounts (equation (1)) of $InCl_3$ (Fluka, purity 98.0%) and $SbCl_3$ (Aldrich Chemical, purity 99.0%) in ethylene glycol (EG, JT. Baker, purity 99.0%) at room temperature. Zinc powder (Fluka, 45μm particle size) was gradually added to the solution. The reaction was continuously stirred for over 1 hour before it was filtered and washed by methanol (Merck, commercial grade). Finally, it was dried in the oven at 65°C for 30 minutes.

$$InCl_3 + SbCl_3 + 3Zn \rightarrow InSb + 3ZnCl_2 \qquad (1)$$

As received product powder was characterized for the phases presented by powder X-ray diffraction (XRD, siemen D500/D501, Cu Kα (λ1.54) Ni filter, 2θ = 10-80°, step:0.02°, step time: 1s) technique. Scanning Electron Microscopy (SEM) equipped with Energy Dispersive Spectroscopy (EDS) (JEOL JSM-6335F) technique was used to observe morphology of the product powders. Finally, nanometer scale morphology which directly related to the crystallography of the phase presented was determined by Transmission Electron Microscopy (TEM) equipped with Energy Dispersive Spectroscopy (EDS) (JEOL JEM-2010) technique.

Results and Discussion

The powder XRD pattern of the as received product was presented in figure 1. There were three phases present; InSb, Sb metal (space group R-3m), and In metal (space group I4/mmm). By applying direct comparison method, the volume fractions of those phases were calculated using the integrated intensities of InSb (111), Sb (012), and In (101) peaks [8]. The intermetallic InSb was observed to form 48% by

volume followed by Sb and In which were observed to appear 34% and 18% by volume, respectively. Small amount of InSb phase presence may possibly be explained by the insufficient electrons moving energy due to low temperature reaction, additionally metals phase presented consequently. However, annealing the product powder at 400°C under argon atmosphere can improve the intermetallic formation approximately 82% InSb, 16% Sb, and 2% In_2O_3 [5,7]. The existence of In_2O_3 was considered as due to the reaction between indium metal and the unremoved ethylene glycol solvent [5].

The morphology of the as received product observed by SEM technique was shown in figure 2. Dendrite structure with an average of 0.84-2.00 μm primary arms, 0.16-0.40 μm secondary arms, and 40-100nm ternary arms was discovered. Because of individual nanometer particle attached to each other creating a specific dendrite structure, the surface area was understood to be relatively high. This property is one of the key parameters needed for fast cell reaction and good capacity retention as well as long charge-discharge cycle life due to proportional of the particle size to the absolute dimensional changes [9-10]. The identification of dendrites was confirmed by TEM studied. The selected area diffraction (SAD) pattern taken from the dendrite particle indicated in figure 3 was indexed as zinc-blende InSb compound. From the preliminary studied, dendrites with lighter color were additionally determined as antimony metal [5]. It is interesting that high crystallinity intermetallic InSb dendrites can amazingly occur at this low temperature, which takes an advantage over other method by lowering the cost of electrode material manufacturing. It also was attractive to note that growing of secondary arms was determined to be 60° angle from primary arms as well as between ternary and secondary arms. The crystallographic growth direction of the primary arm was measured to be [220]

direction. The mechanism of dendrite formation was proposed [5-6] as a nucleation of the intermetallic compounds on the reducing agent particles and finally grown into dendrites. After zinc powders had all transformed into ions, detached dendrite particles were found to disperse in the solution.

The electrochemical properties of the annealed material were reported previously [7] to provide approximately 400 mAh g^{-1} in the first cycle and drop to 350 mAh g^{-1} in the second cycle followed by slow capacity fading in the subsequence cycles. The large irreversible capacity in the first cycle and capacity fading were assumed as due to Sb and In_2O_3 impurities. The electrochemical performance of this material can be improved by minimizing those impurities. Processing parameters, such as solvent type, reducing agent, reaction temperature, and more importantly reacting under inert gas atmosphere are all necessary parameters that need to be controlled in order to receive the most suitable mean to produce high purity InSb compound.

Conclusion

The binary semiconducting compound, InSb can be synthesized by solution route method with In and Sb impurities. Crystalline dendrite morphology of InSb powders were received from this method. It was considered to provide high surface area suitable for making lithium-ion batteries negative electrode. However, the small amount of impurities presence affected the cell performance. Therefore, the synthesis method improvements are strongly necessary to minimize those contaminations.

Acknowledgement

The Chiang Mai University electron microscopy research and service center is thanked for sample testing. Supported for this work from the Thailand Research Fund (TRF) and The Commission on Higher Education, contract no MRG4680166 is gratefully acknowledged.

References

[1] C. S. Johnson, J. T. Vaughey, M. M. Thackeray, T. Sarakonsri, S. A. Hackney, L. Fransson, K. Edstrom, J. O. Thomas, Electrochemistry and in-situ X-ray diffraction of InSb in lithium batteries, *Electrochemical Communications* 2 (2000) 595-600

[2] J. T. Vaughey, J. O'Hara, and M. M. Thackeray, Intermetallic insertion electrodes with zinc blende-type structure for Li Batteries: A study of Li_xInSb ($0 \leq x \leq 3$), *Electrochemical and Solid State Letters*, 3 (2000) 13

[3] M. M. Thackeray, C. S. Johnson, A. J. Kahaian, K. D. Kepler, J. T. Vaughey, Y. Shao-Horn, S. A. Hackney, Composite electrodes for lithium batteries, *ITE Battery Letters* 1(1) (1999) 26

[4] R. Janot, D. Guérard, *Progress in Materials Science* 50 (2005) 1-92

[5] T. Sarakonsri, *On the processing and properties of binary compound insertion electrodes*, Ph.D. Thesis, Michigan Technological University, Houghton, USA (2002).

[6] T. Sarakonsri, T. Apirattanawan, S. Tungprasurt and T. Tunkasiri, Solution synthesis of dendrite Cu6Sn5 powders, anode materials for lithium-ion battery, Submitted to *Journal of Materials Science*

[7] T. Sarakonsri, C. S. Johnson, J. T. Vaughey, N. Li, S. A. Hackney, and M. M Thackeray, Low temperature synthesis of intermetallic and composite electrodes for lithium batteries, presented at *12th International Meeting on Lithium Batteries (IMLB-12)*, Nara, Japan, June 27-July 2, 2004

[8] B. D. Cullity, *Elements of X-ray Diffraction*, 2nd ed. (Massachusetts, Addison-Wesley, 1977)

[9] O. Mao, R. L. Turner, I. A. Courtney, B. D. Frederickson, M. I. Buckett, L. J. Krause, and J. R. Dahn, Active/inactive nanocomposites as anodes for li-ion batteries, *Electrochemical and Solid-State Letters*, 2(1) (1999) 3-5

[10] J. Yang, Y. Takeda, N. Imanishi, J. Y. Xie, O. Yamamoto, Intermetallic $SnSb_x$ compounds for lithium insertion hosts, *Solid State Ionics* 133 (2001) 189-194

Figure Captions

Figure 1 Powder XRD pattern of the as received product

Figure 2 SEM micrograph of the as received product powders showing dendrite morphology

Figure 3 TEM micrographs showing the dendrite particles (a) and the dendrite tip with the inserted single crystal SAD pattern corresponds to InSb phase (b)

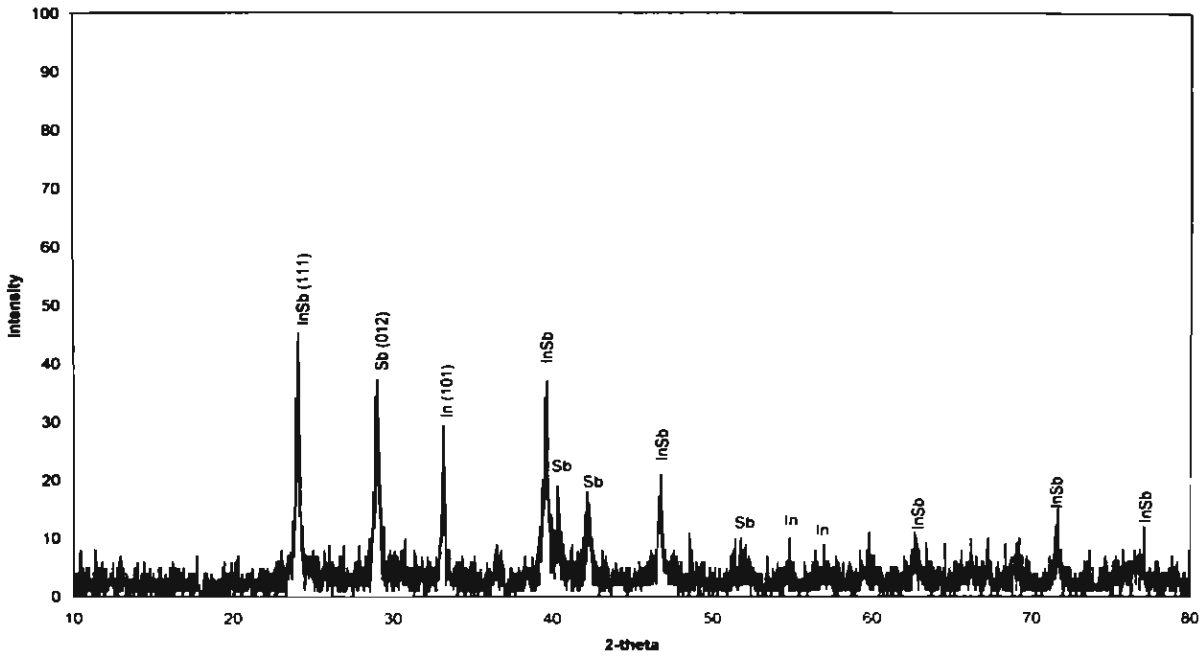
Intensity
2-theta
InSb (111)
Sb (012)
In (101)
InSb
Sb
Sb
InSb
Sb
In
In
InSb
InSb
InSb

Figure 1

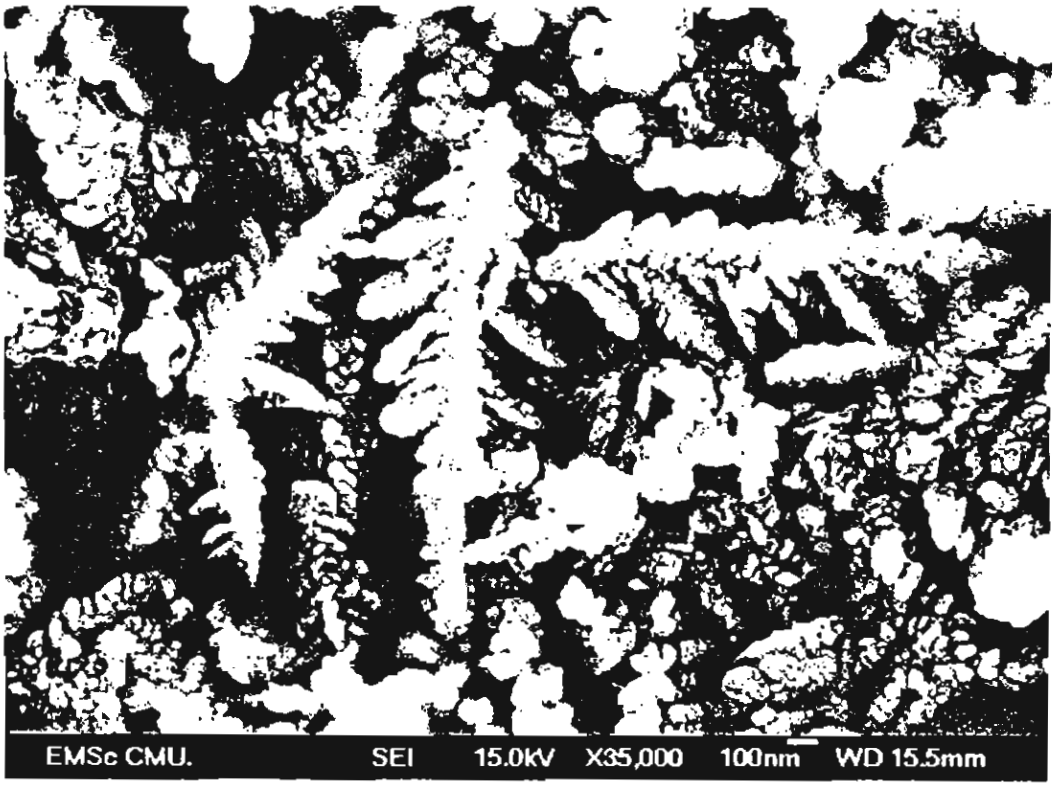

Figure 2

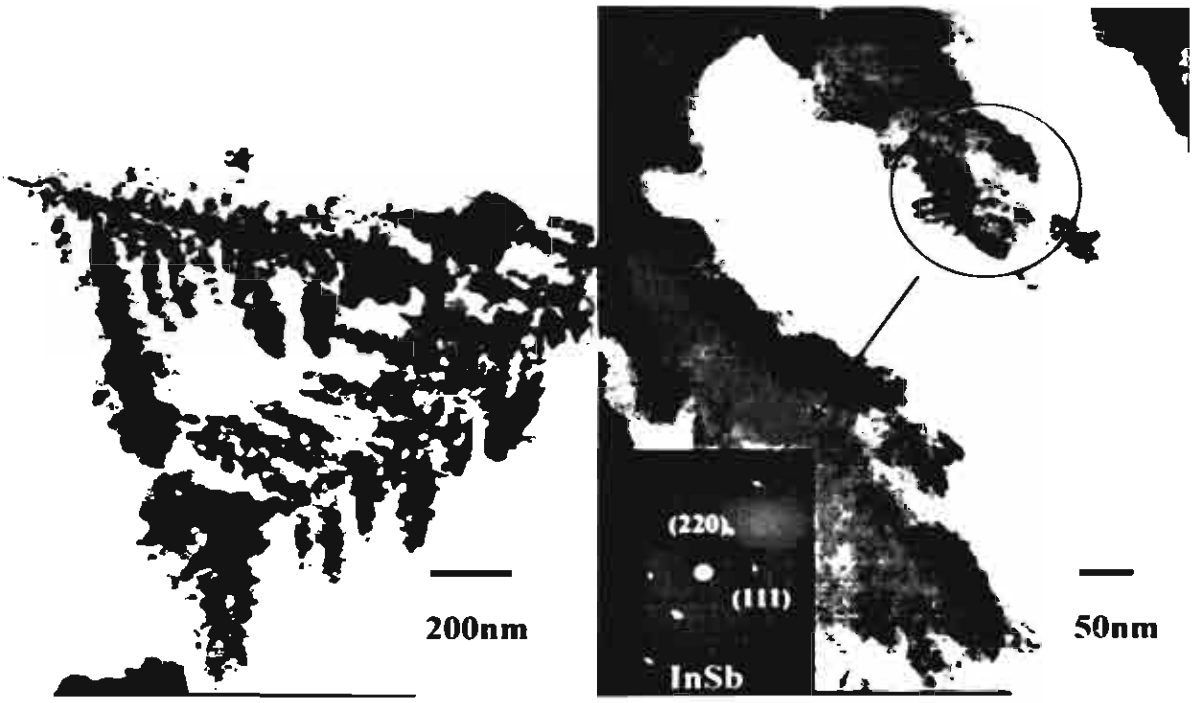

Figure 3

Electron microscopy study of the formation of dendrite Cu_6Sn_5 powders, synthesized by solution route method

S. Thungprasert[a*], T. Sarakonsri[a**], and T. Tunkasiri[b]

[a]Department of Chemistry, Chiang Mai University, Chiang Mai 50200, Thailand

[b]Department of Physics, Chiang Mai University, Chiang Mai 50200, Thailand

Abstract

Dendrite Cu_6Sn_5 powders, a potential anode material for lithium-ion battery, can be synthesized by performing a redox reaction between stochiometric amount of metals chlorides and zinc metal in ethylene glycol solvent. The formation of dendrite morphology was investigated by considering two processing parameters. Two forms of reducing agent; zinc powders (45 μm) and zinc plate, were the first parameter. Reaction time varying from 1-5 minutes was the second one. From the characterization of the product powders by using SEM and TEM techniques, Cu_6Sn_5 compound was discovered to nucleate on reducing agent particles and subsequently grown into dendrite structure with long branches. These results have confirmed the proposed mechanism for dendrite formation in this solution system.

Keywords; Cu_6Sn_5, lithium-ion battery, synthesis, dendrite structure, and electron microscopy

---

* Corresponding author. Email address: siwattawis@yahoo.com

** Corresponding author. Tel: +66-53-941907; Fax: +66-53-892277

Email address: scchi017@chiangmai.ac.th

Introduction

A lithium-ion battery is an important portable power source for the current human society because of its high energy density, high voltage, long cycle life, flexible design and considerably safe to use [1]. Lithium-ion batteries were developed to replace Ni-Cd batteries which contain toxic materials and encounter a problem on memory effect [2]. Lithium-ion batteries commercially made from graphite negative electrode, which gave excellent cycle ability without memory effect problem [3]. However, there is a safety concern due to lithiated graphite, Li_xC_6, reach the lithium potential when cells approach a fully charged state as the positive electrode ($Li_{1-x}CoO_2$) was a highly oxidizing agent [4]. Moreover, it provides volumetric capacity only about 750 mAh/cm^3 [3]. The Cu_6Sn_5 compound, then was proposed as an intermetallic insertion negative electrode due to their high volumetric capacity (approximately 1760 mAh/cm^3) over graphite electrode and it reacted with lithium at the voltage above 100 mA, which satisfy the safety issue [5,6].

The Cu_6Sn_5, which initially has NiAs type structure, can be rearranged itself into zinc-blende type structure after the first discharge [7]. The initial-research reported that Cu_6Sn_5 compound could be synthesized at low-temperature by the solution route method [8], which also can be used to synthesize other intermetallic compounds. The morphology of the intermetallic powders was studied and reported to have dendrite structure [8]. The dendrites, which had branches composed of nanometer size particles, were considered to have relatively high surface area compared with the material synthesized by mechanically alloying. The dendrite structure also could be synthesized by another methods such as solvothermal or hydrothermal [9,10]. These two methods produce nanoscale dendrite structure similar to solution route method. However, it takes longer time to synthesize. Solution route method then was a convenience and easy controlled method, which was applied to follow the formation of dendrite in a short period of time.

As was reported initially, the dendrite morphology was proposed to occur by the "point effect of the electric field" [8]. This research therefore has applied electron microscopy techniques which were scanning electron microscopy (SEM) and transmission electron microscopy (TEM) to investigate the dendrite formation and to prove the above hypothesis. Different forms of zinc reducing agent, which were zinc powders and zinc plates, were studied in this experiment. The plate shape reducing agent was used because the dendrite development will be easily observed due to larger particle, which associated with high electron density, compared with powder reducing agent. Reaction time was an important parameter for the study of dendrite formation mechanism. Products examination after the reaction occurred for 1,2,3,4, and 5 minutes allowed the dendrite development to be observed.

Experimental

The experimental procedure was conducted as followed. The experimental condition was described by dissolving stoichiometric amounts (equation (1)) of $CuCl_2$ (Sigma-Aldrich, purity 99.0%) and $SnCl_2$ (Sigma-Aldrich, purity 99.0%) in ethyl glycol (JT. Baker, purity 99.0%) at room temperature. The metal ions were reduced by adding zinc powder (Fluka, 45 μm particle size) and the reaction was stirred for 1 minute. Then, the product powder was filtered and washed by methanol (Merck, commercial grade). Finally, it was dried in the oven at 65 °C for 30 minutes. The subsequence experiments were performed analogues to the above experiment except varying reaction times to 2 and 5 minutes. Other reactions were carried out the same as all the above experiments except using zinc plate (Riedel-deHën, purity 99.9%) as reducing agent and varying the reduction times by 1,2,3,4, and 5 minutes.

$$6CuCl_2 + 5SnCl_2 + 11Zn \rightarrow Cu_6Sn_5 + 11ZnCl_2 \qquad (1)$$

The dendrite formation at different reaction times then was studied by Scanning Electron Microscopy (SEM, JEOL JSM-6335F) technique. The nanometer scale morphology was observed to confirm the SEM results using Transmission Electron Microscopy (TEM, JEOL JEM-2010) technique.

Result and discussion

Initially, the SEM technique was employed for morphology study. The pre-reacted zinc powders was observed as smooth surface and had particle size around 30-50 μm (figure 1a). At 1 minute reaction, the SEM micrograph in figure 1b shows that the zinc particlewas partly covered by a large number of small dendrites. The small size of dendrite particles were observed due to only a few electrons were transferred to copper and tin ions for copper tin compound formation. At 2 minutes reaction, the dendrite particles were found to fully cover the zinc particle (figure 1c). The mechanism of dendrite formation can possibly be considered to occur initially by the Cu_6Sn_5 intermetallic compound on the zinc surface had formed in group of lump and subsequently grown out into dendrites by the prefer transferring path of electrons from zinc through intermetallic compound rather than transferring to distributed ions in the solvent. The possible reason as was proposed, due to there was the electrochemical overpotential at the solution precipitate interface that produce an electric field and act as electrodes for the reduction of the Sn and Cu ions at the dendrite tip. Intermetallic compound therefore, has grown out as branches from lump to dendrite structure (figure 2) by the "point effect of the electric field" mechanism. The electrons from zinc particles had transferred through intermetallic compound to metal ions in solvent at the top of

branches. At 5 minutes reaction (figure 1d), the dendrites grown into complete dendrite and were dispersed in the solution due to the disappearance of zinc metal. It was observed at the end that the groups of dendrite particle were dispersed in the solution by the stirring process and some dendrites had broken into small branches.

The characterization by TEM technique gave similar results to SEM technique. As shown in figure 3a and 3b for the product synthesized for 1 minute. The light color particle attached to dendrite at the bottom left corner was confirmed by poly crystal selected area diffraction (SAD) pattern to be zinc metal. It was noted that more spots in SAD pattern similar to ring pattern were observed in figure 3b due to large zinc particles presence. Therefore, the TEM results consistence with SEM results which verified the number of dendrite structures from zinc particle and the growing of their branches by the proposed mechanism.

For the reaction using zinc plate reducing agent, the SEM image of the pre-reacted zinc plate is shown in figure 4a. The SEM image of the product from 1 minute reaction was shown in figure 4b along with the SEM image of the products from 2, 3, 4, and 5 minutes reaction in figure 4c-4f, respectively. At 1 minute reaction, zinc plate bonded the group of lump on it surface. Similar results as for zinc powders condition were observed, except no dendrite structure formed on the zinc surface because of the electrons transferring from zinc to metal ions for zinc powders were better than for zinc plate condition. Its reason which can be described as due to the presence of an oxide film on the zinc plate surface, which was a good oxidizing agent, snatched electrons from copper and tin ions and consequently decease growing rate of intermetallic compound. Then, the dendrites were observed to grow into longer branches at 2 minutes reaction time and continue to grow extensively as the time increase. Compared with the previous zinc

powder condition, larger dendrites were formed by using zinc plate because of an infinite number of electrons provided for the reduction process.

This research has also discovered that the number of dendrites at 1 minute reaction time from the zinc powder condition were relatively higher than those from the zinc plate condition. This phenomenon con be explained by the possibility of the impurity such as oxide film on the zinc plate surface hindrance the dendrite nucleation. On the other hand, at 5 minutes reaction, the dendrites from the zinc plate condition had relatively longer branches than those from the zinc powders condition. The reason was due to the insufficient electrons from zinc powder for extended grown of dendrites and the reduction process completed before it reached 5 minutes. Therefore, separated dendrites were found randomly in the solution.

Conclusion

The dendrite Cu_6Sn_5 powder can be successively synthesized by solution route method. The formation of Cu_6Sn_5 dendrite was effectively monitored by examining the products at different reaction times using SEM and TEM techniques. Different froms of zinc reducing agent were employed to reveal the dendrite formation behavior. The proposed nucleation mechanism by "point effect of the electric field" was confirmed to occur in this solution route method.

Acknowledgement

CMU electron microscopy research and service center is thanked for sample testing. Supported for this work from the Thailand Research Fund (TRF) and The Commission on Higher Education, contract no MRG4680166 is gratefully acknowledged.

Reference

[1] L.M.L. Fransson, J.T. Vaughey, R. Bendek, K. Edström, J.O. Thomas and M.M. Thackeray, Electrochemistry Communications 3 (2001) 317-323.

[2] B.Ramachandra Reddy, D. Neela Priya, S. Venkateswara Rao, P. Radhika , Hydrometallurgy 77 (2005) 253-261.

[3] Shoufeng Yang, Peter Y. Zavalij, M. Stanley Whittingham, Electrochemistry Communications 5 (2003) 587–590.

[4] D. Kepler, J.T. Vaughey, and M.M. Thackeray, Electrochemical and Soild-State Ioincs, 90 (1996) 281.

[5] M.M. Thackeray, C.S. Johnson, A.J. Kahaian,, K.D. Kepler, J.T. Vaughey, Y. Shao-Horn, S.A. Hackney, ITE Battery Letters Vol. 1, No.1

[6] M.M. Thackeray, J.T. Vaughey, A.J. Kahaian, K.D. Kepler, R. Benedek, Electrochemistry Commusication 1 (1999) 111-115

[7] J.T. Vaughey, K.D. Kepler 1, R. Benedek, M.M. Thackeray, Electrochemistry Communications 1, 1999, 517–521.

[8] T. Sarakonsri, T. Apirattanawan, S. Tungprasert, T. Tunkasiri, summitted to J. Materials Science.

[9] Hanmei Hu, Baojun Yang, Qiaowei Li, Xinyuan Liu, Weichao Yu, Yitai Qian, Journal of Crystal Growth 261 (2004) 485–489.

[10] Yongchun Zhu, Huagui Zheng, Yuan Li, Lisheng Gao,Zhiping Yang, Yitai Qian, Materials Research Bulletin 38 (20 03) 1829–1834.

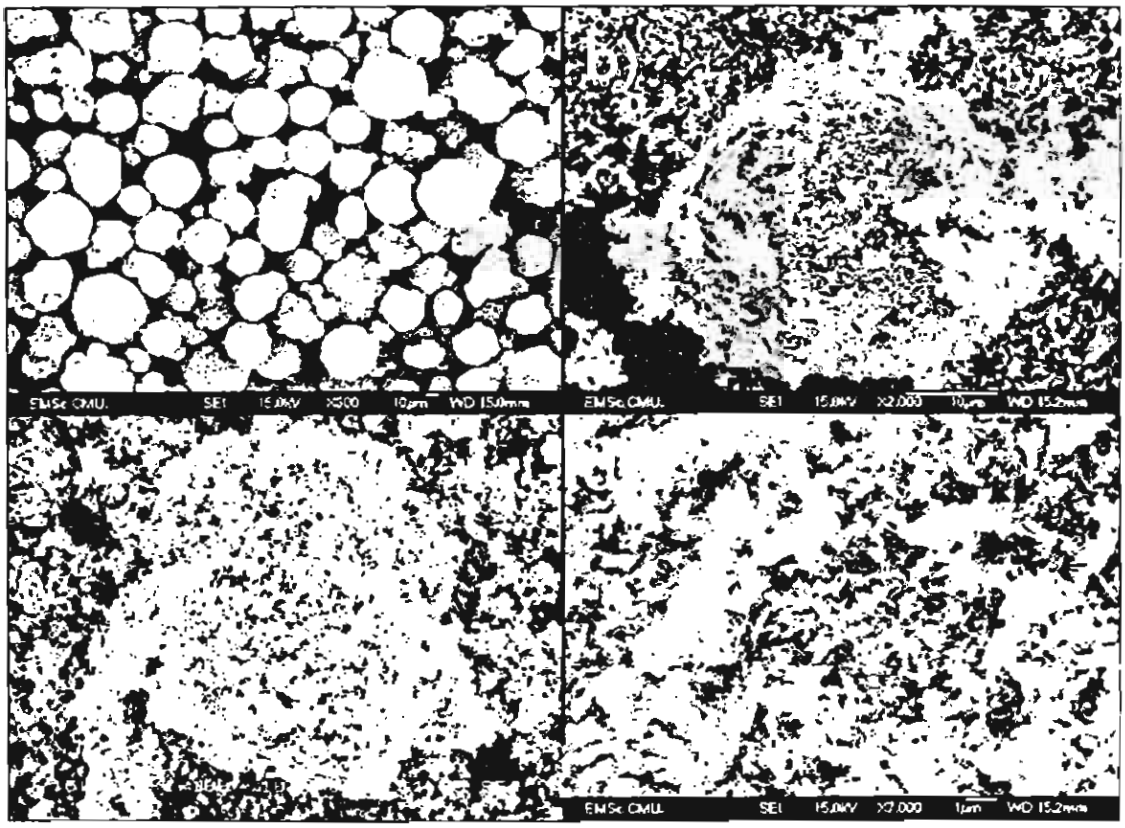

Figure 1 SEM micrographs showing the pre- reacted zinc powders (a) Cu_6Sn_5 dendrites on zinc powder at 1 minute (b), 2 minutes (c), and 5 minutes reaction time (d).

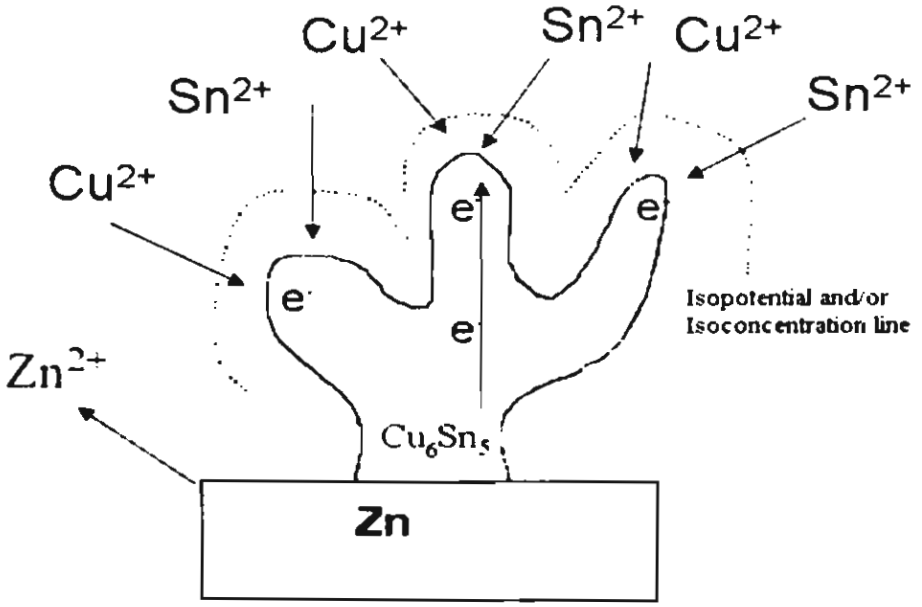

Figure 2 Schematic diagram of the nucleation mechanism of dendrite Cu_6Sn_5 on zinc particle.

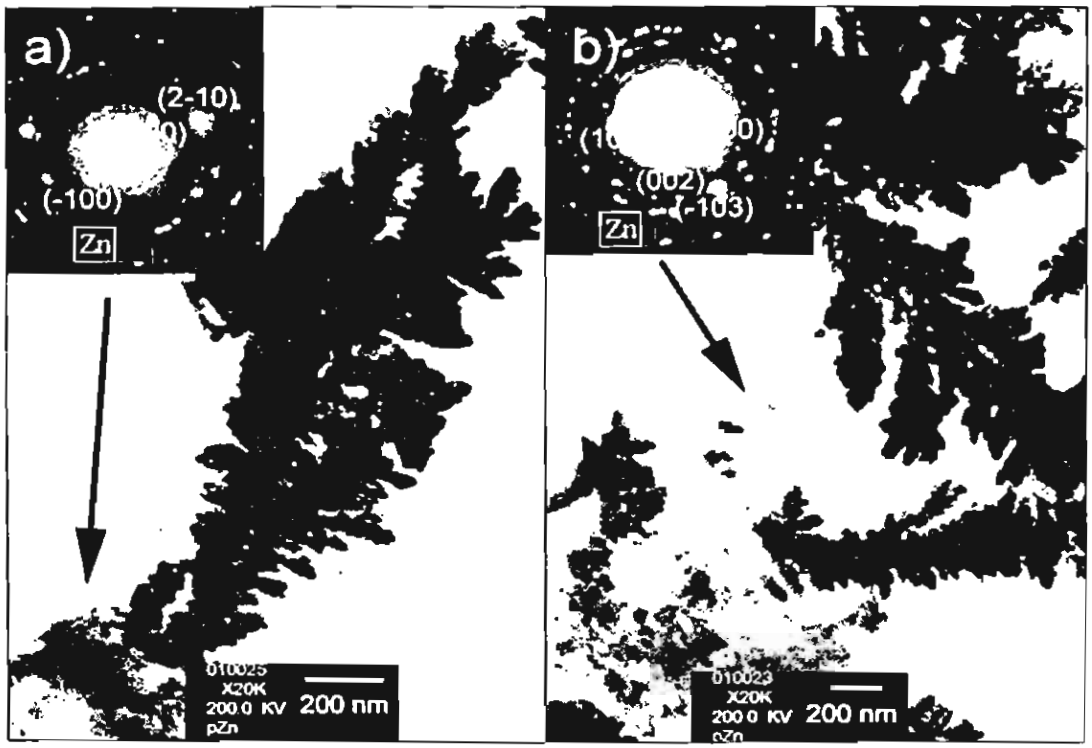

Figure 3a and 3b TEM micrographs of Cu_6Sn_5 dendrite particles attached to zinc powder and the corresponding zinc diffraction patterns from 1 minute reaction time in the inserted figures.

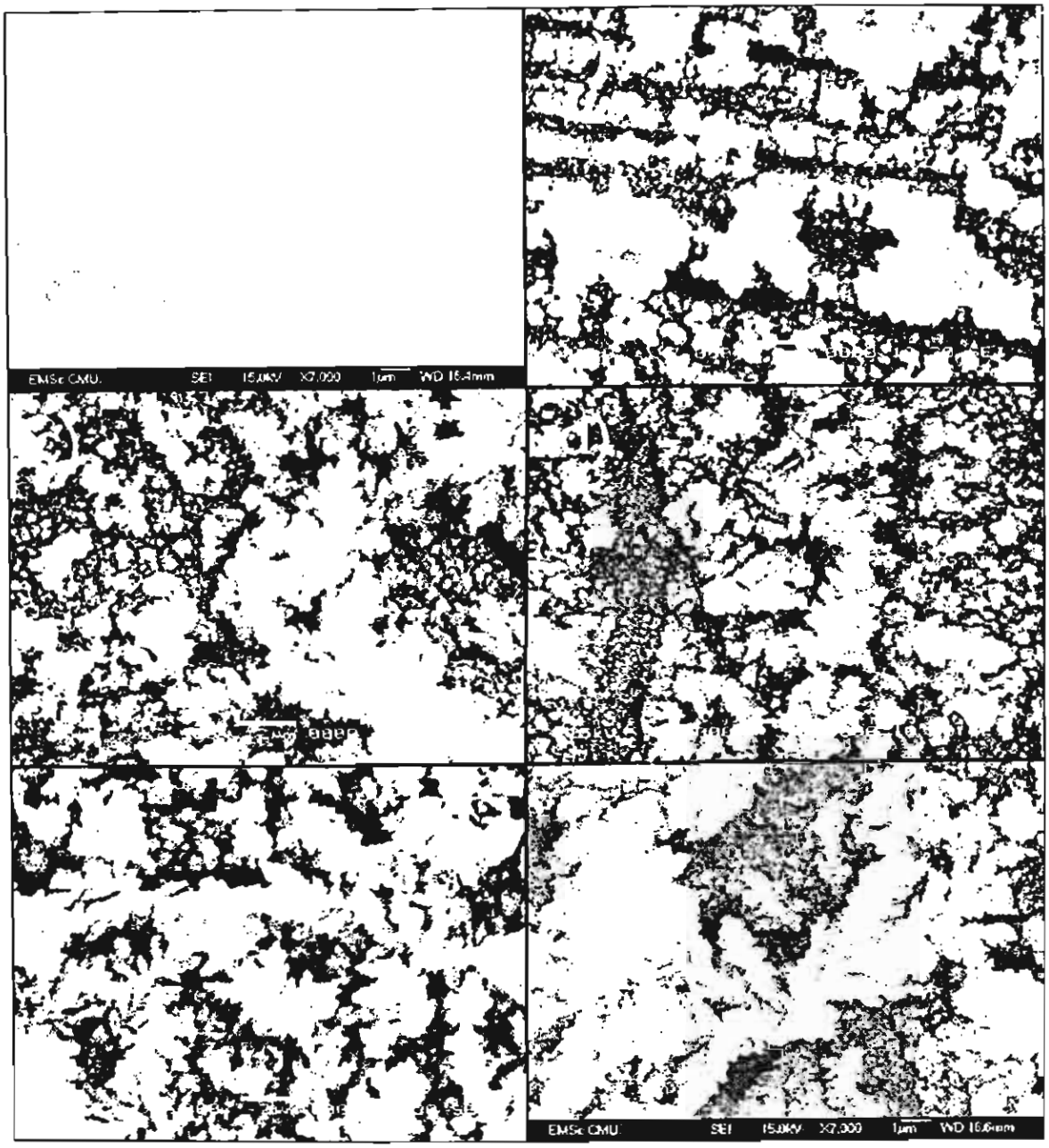

Figure 4 SEM micrographs showing the pre-reacted zinc plate surface (a), Cu_6Sn_5 dendrites on zinc plate at 1 minute (b), 2 minutes (c), 3 minutes (d), 4 minutes (e), and 5 minutes reaction times (f).